Development of Nonlinear Elastic Bending and Torsion of Articulated Rotor Blades With an Impedance Control Device Replacing The Common Pitch Link

Derek Gransden[i], Mehrdaad Ghorashi[ii],
Robert Langlois[iii], and Fred Nitzsche[iv]
Department of Mechanical and Aerospace Engineering, Carleton University
Ottawa, Canada

Abstract

In this paper, the time-dependent non-linear partial differential equations of motion for both cantilever and articulated rotorcraft blades are derived based on a Newtonian approach. In the former case, the initial-boundary value problem is solved using linearized equations, via a central finite difference method. Deflection, bending moment, and shear force distributions during the vibration have been obtained. Included in the latter case is a semi-active impedance control device that attenuates higher-harmonic vibration transmitted from the blade to the rotorcraft frame. This device reduces the transmissibility ratio by replacing the pitch link and controlling the boundary conditions at the root of the blade. Based on the system state, the controller device engages or disengages the piezoelectric actuators that change the effective mass and stiffness. In this way, the elastodynamic system is complicated further by time-variant boundary conditions. Further research is currently in progress in order to evaluate the effect of the proposed control system on reducing the blade-frame transmissibility ratio.

Nomenclature

A	Cross-section area	k	Spring stiffness
$\vec{a}$	Acceleration vector	k_A^2	Polar radius of gyration
A_n	Transformation matrix from A_{n-1} to A_n frames of reference	k_m^2	Torsional mass moment of inertia
		$k_{m_1}^2, k_{m_2}^2$	Principal mass moments of inertia
B_1	Blade cross-section integral	L	Pitch link offset
B_2	Blade cross-section integral	l	Fixed length between revolute joints
C	Product used in control algorithm	$\vec{M}$	Moment vector (M_x, M_y, M_z for undeformed co-ordinates)
c	Chord length		
C_1	Second sectorial moment (warping constant, $I_{\lambda\lambda}$)	m	Mass per unit length
		N	Normal force from control device
C_1^*	Second sectorial moment ($I_{\lambda\eta}$)	n	Co-ordinate frame number
d	a) Pitch horn length	P	Distance to blade from pitch hinge
	b) Variable length between joints	$\vec{p}$	Body force vector (p_x, p_y, p_z)
E	Young's modulus	P_i	Length between pitch horn and hinge
e	Center of mass axis offset from elastic axis	P_o	Length between pitch horn and blade edge
$E*$	Flap hinge offset	$P_{x'}$	Warping restraint boundary condition
e_A	Tension axis offset from elastic axis	$\vec{q}$	Body moment vector (q_x, q_y, q_z)
F	a) Lag hinge offset	r_p	Generic point on blade $r_p = (x_p, y_p, z_p, 1)$
	b) Force from impedance control device	T	Kinetic energy term in Hamilton's principle
F_f	Friction force from control device	t	Time variable
G	Shear modulus	T_{bl_o}	Torque on blade (M_x in derivation)
$I_{y'}, I_{z'}$	Moments of inertia (deformed co-ordinates)	U	Strain energy term in Hamilton's principle
J	Torsion constant	u	Axial deflection
		$\vec{V}$	Force vector (V_x, V_y, V_z for

[i]Research Assistant.
[ii]Post-Doctoral Fellow.
[iii]Associate Professor.
[iv]Professor. Corresponding author: Fax: +(613) 520-5715; Email: fred_nitzsche@carleton.ca

	undeformed co-ordinates)
v	Lag deflection
$\bar{v}$	Non-dimensional lag deflection
$\vec{v}$	Velocity vector
W	Non-conservative work
w	Flap deflection
$\bar{w}$	Non-dimensional flap deflection
X	Inertial x-direction (pos. aft)
$\bar{x}$	Non-dimensional blade x position
x_i	Co-ordinate frame i x-direction
Y	Inertial y-direction (pos. starboard)
y_i	Co-ordinate frame i y-direction
Z	Inertial z-direction (pos. up)
z_i	Co-ordinate frame i z-direction
α	T_6 skew line angle
β	Flap hinge angle
Δt	Time step in finite difference scheme
Δx	Length of element on blade in finite difference scheme
ϵ	Engineering strain
ζ	Lead-lag hinge angle
η	Blade major principal axis co-ordinate
θ	a) Commanded pitch angle
	b) T_6 rotation variable
λ	a) Warp function
	b) State space variable
λ_η	Derivative of warp function with respect to chord co-ordinate
λ_ξ	Derivative of warp function with respect to thickness co-ordinate
ξ	Blade minor principal axis co-ordinate
ρ	Density
σ	Engineering stress
ϕ	Aeroelastic pitch angle
ψ	Azimuth angle
$(\ )'$	Spatial derivative along blade length
$(\dot{\ })$	Time derivative
a	(Subscript) Denotes actuating body
bl	(Subscript) Denotes blade system
c	(Subscript) Denotes controlled body
i	(Subscript) a) Denotes i-axis $(i = x, y, z, \eta, \xi)$
	(Subscript) b) Denotes space variable in finite difference scheme
i'	(Subscript) Deformed i-axis $(i = x, y, z)$
ss	(Subscript) Denotes impedance control device
Vol	(Subscript) Denotes volumetric properties
I	(Superscript) Denotes inertial frame reference
j	(Superscript) Denotes time variable in finite difference scheme

Introduction

The study of active control techniques to reduce the aerodynamically induced vibrations of rotor blades is a principal subject of current research. In order to solve this problem, the nonlinear dynamic equations governing the vibration of the active rotor blade system have to be established. Two of the early reports that have focused on the passive analysis of rotor blade dynamics are those of Refs 1 and 2. In these references, the nonlinear elastodynamic behaviour of hingeless rotor blades has been formulated using beam theory. More recent research in the same area includes that of Refs 3 to 7. Apart from the structural dynamic and aeroelastic analyses, active vibration control has also become a main focal point of research. This is exemplified by the recent works presented in Refs 8 and 9. Most of the mentioned contributions discuss the case of hingeless rotor blades.

The current research is an attempt to present a method for vibration control of fully articulated rotorcraft blades and utilizes an impedance control idea that was presented in Ref 10. A semi-active impedance control device is introduced as a substitute for the usual pitch link to attenuate the higher-harmonic vibrations transmitted from the helicopter blade to the swash plate. The elastodynamic behaviour of an articulated rotor blade implementing the impedance control device is formulated.

From a dynamics point of view, the articulation changes the kinematics of the blade by including rigid body motions. Therefore, the linkage system results in different acceleration expressions for arbitrary points on the articulated blade compared to the hingeless blade. This, in turn, results in a set of inherently different body forces and moments for the hinged blade.

In the present paper the dynamics of a rotating uniform blade, with both hinged and hingeless configurations, made of a homogeneous isotropic material is discussed. The cross-section of the blade is assumed to be symmetrical with respect to the chordal axis, i.e., the η-axis. After the problem is formulated, the corresponding non-dimensional form of the equations
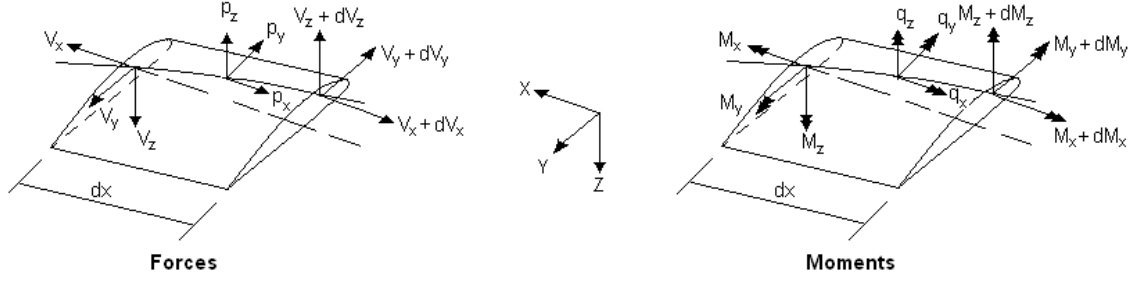
Figure 1: Inertia forces and moments, together with induced internal forces and moments

is linearized and simplified to the non-articulated case. Consequently, in order to validate the general equations for a specific case, they are compared to the existing literature on cantilever rotor blades. Next, the response of the non-articulated rotor blade system in the hovering flight condition is analyzed using the finite difference method. To obtain results verifiable from literature and simulations from other elastodynamic models, the analysis does not include the impedance controller. This case will be followed by future analysis of the fully articulated blade model.

Elastodynamic Equations of the Blade

Utilizing D'Alembert's principle for the dynamic equilibrium of an infinitesimal blade element, dx, loaded as shown (Fig 1), the equations of motion are

$$\frac{\partial \vec{V}}{\partial x} + \vec{p} = 0 \qquad (1)$$

and

$$\frac{\partial \vec{M}}{\partial x} + \vec{i'} \times \vec{V} + \vec{q} = 0 \qquad (2)$$

Equations (1-2) can be combined to eliminate the dependency on V_y and V_z such that the three moment equations and one force equation become

$$\frac{\partial M_x}{\partial x} + \left(\frac{\partial M_y}{\partial x} + q_y\right)\frac{\partial v}{\partial x} + \left(\frac{\partial M_z}{\partial x} + q_z\right)\frac{\partial w}{\partial x} + q_x = 0$$

$$\frac{\partial^2 M_y}{\partial x^2} + p_z + \frac{\partial}{\partial x}\left(V_x \frac{\partial w}{\partial x}\right) + \frac{\partial q_y}{\partial x} = 0 \qquad (3)$$

$$\frac{\partial^2 M_z}{\partial x^2} + p_y + \frac{\partial}{\partial x}\left(V_x \frac{\partial v}{\partial x}\right) + \frac{\partial q_z}{\partial x} = 0$$

$$\frac{\partial V_x}{\partial x} + p_x = 0$$

The appropriate co-ordinate frame transformation between the deformed and undeformed axis systems is given in Ref 2. The same transformation holds true for the x, y, and z components of forces and moments. Eliminating the higher order terms, the first of Equations (3) results in

$$M'_{x'} - M_{y'}[v'' \cos(\theta + \phi) + w'' \sin(\theta + \phi)]$$
$$+ M_{z'}[v'' \sin(\theta + \phi) + w'' \cos(\theta + \phi)] \qquad (4)$$
$$+ q_x + v' q_y + w' q_z = 0$$

The other two moment equations in (3) can also be simplified further since the product of the torque $M_{x'}$ and a deflection slope v' or w' may be ignored compared to the moments $M_{y'}$ and $M_{z'}$. This is because the chord length is considerably smaller than the rotor length, so a point force on the rotor blade will have a smaller moment arm for producing torques than for bending moments. If the torque applied is small compared to the applied bending moments,

$$q_x \ll q_y, q_z$$

by integrating the latter two moment equations in (3) and multiplying them by the slopes of the deflections, then subtracting the result from the mentioned moment equations, the terms $M_{x'}v'$ and $M_{x'}w'$ can be eliminated. The additional terms introduced by these operations are negligible compared to the second order loading
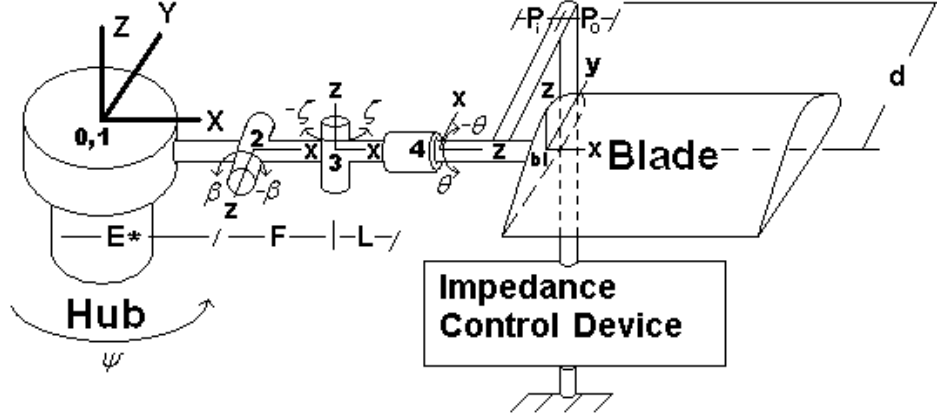
Figure 2: Helicopter rotor blade geometry

terms, q_y and q_z, and therefore the two moment equations from (3) can be rewritten as

$$[M_{y'} \cos(\theta + \phi) - M_{z'} \sin(\theta + \phi)]'' + (V_x w')'$$
$$+ p_z + q_y' = 0 \qquad (5)$$
$$[M_{y'} \sin(\theta + \phi) + M_{z'} \cos(\theta + \phi)]'' - (V_x v')'$$
$$- p_y + q_z' = 0$$

If the tension in the helicopter blade changes significantly, an equation for $V_{x'}$ from the nominal centripetal force caused by the blade rotation is required as a function of the rotor blade deformation. Transforming the forces from Equation (1) to the deformed axis system and by substituting $V_{y'}$ and $V_{z'}$ for $V_{x'}$ into the deformed Equation (3), and neglecting the higher order terms, $V_{x'}$ becomes

$$V_{x'} = \int_x^R p_x \, dx + v' \int_x^R p_y \, dx + w' \int_x^R p_z \, dx \quad (6)$$

Thus, the principal expressions for the moment equilibrium, i.e. Equations (4) and (5), combined with Equation (6) for force equilibrium, describe the internal and external moments and forces acting on the blade. For helicopter applications, the terms of third order or higher are negligible compared to those of second order, and therefore, $V_{x'} = V_x = T$.

To satisfy dynamic equilibrium, the summation of the inertial, internal, and external loadings is zero. To evaluate this, the inertial expressions, the stress-strain relationships, and the aerodynamic loads must be obtained. Then the boundary conditions may be formulated to provide the necessary equations to solve the mathematical formulation.

Inertial Loading   The position vector of an arbitrary point on the rotorcraft blade is

$$\vec{r}_p = \begin{bmatrix} x + u - \lambda\phi' - v'[\eta\cos(\theta + \phi) - \xi\sin(\theta + \phi)] \\ -w'[\eta\sin(\theta + \phi) + \xi\cos(\theta + \phi)] \\ \\ v + \eta\cos(\theta + \phi) - \xi\sin(\theta + \phi) \\ \\ w + \eta\sin(\theta + \phi) + \xi\cos(\theta + \phi) \\ \\ 1 \end{bmatrix}$$

However, for an articulated helicopter blade, a generic point on the blade must be transformed to the hub co-ordinate frame before any inertial loads can be calculated. Based on Fig 2, and following the methodology described in Ref 11 for the rotor mechanism, the Denavit-Hartenburg (D-H) parameters are indicated in Table 1.

Table 1: D-H Parameters

n	θ_n	d_n	l_n	α_n
1	ψ	0	0	0
2	0	0	$E*$	$\frac{\pi}{2}$
3	β	0	F	$-\frac{\pi}{2}$
4	$\frac{\pi}{2} + \zeta$	0	0	$\frac{\pi}{2}$

These values are then input into the following D-H matrix, which describes the transformation

between the $n-1$ and n frames of reference.

$$\mathbf{A_n} =$$

$$
\begin{bmatrix}
\cos\theta_n & -\sin\theta_n\cos\alpha_n & \sin\theta_n\sin\alpha_n & l_n\cos\theta_n \\
\sin\theta_n & \cos\theta_n\cos\alpha_n & -\cos\theta_n\sin\alpha_n & l_n\sin\theta_n \\
0 & \sin\alpha_n & \cos\alpha_n & d_n \\
0 & 0 & 0 & 1
\end{bmatrix}
$$

However, the last frame of reference does not conform to the required orientations of the Denavit-Hartenburg formulation, so it must be calculated separately as follows

$$
\mathbf{A_{bl}} =
\begin{bmatrix}
0 & 1 & 0 & 0 \\
0 & 0 & 1 & 0 \\
1 & 0 & 0 & L+P \\
0 & 0 & 0 & 1
\end{bmatrix}
$$

The final transformation matrix, i.e.,

$$\mathbf{T_6} = \mathbf{A_1 A_2 A_3 A_4 A_{bl}}$$

is given in Appendix A.

Thus, the coordinates of a generic position vector of a point on the blade in the "bl" system shown in Fig 2, pre-multiplied by the transformation matrix, $\mathbf{T_6}$, yields the corresponding position in the inertial frame of reference, $\vec{R}_p$.

$$\vec{R}_p = \mathbf{T_6}\vec{r}_p = \mathbf{A_1 A_2 A_3 A_4 A_{bl}}\vec{r}_p$$

The inertial accelerations are required to determine the inertial forces and moments. The accelerations are calculated by taking the second time-derivative of the inertial position vector, R_p. Now, since the transformation matrix is also time dependent, the following expression is obtained

$$\vec{a}^I = \ddot{\mathbf{T}}_6\vec{r}_p + 2\dot{\mathbf{T}}_6\dot{\vec{r}}_p + \mathbf{T_6}\ddot{\vec{r}}_p$$

The inertial forces and moments can be determined using the expressions stated in Ref 2 as shown below. Note that although the same expressions apply, the resulting inertial forces and moments are not identical due to incongruent definitions of the inertial frames of reference.

$$
\begin{aligned}
p_x^I &= -\iint_A \rho a_x \, d\eta d\xi \\
p_y^I &= -\iint_A \rho a_y \, d\eta d\xi \qquad (7) \\
p_z^I &= -\iint_A \rho a_z \, d\eta d\xi
\end{aligned}
$$

$$
\begin{aligned}
q_x^I &= \iint_A \rho a_y(z_p - w) - \rho a_z(y_p - v)\,d\eta d\xi \\
q_y^I &= -\iint_A \rho a_x(z_p - w)\,d\eta d\xi \qquad (8) \\
q_z^I &= \iint_A \rho a_x(y_p - v)\,d\eta d\xi
\end{aligned}
$$

Where the blade mass constants (used in the final equations) are defined as follows:

$$
\begin{aligned}
m &\equiv \iint_A \rho \, d\eta d\xi \qquad & e &\equiv \frac{1}{m}\iint_A \rho\eta \, d\eta d\xi \\
k_{m_1}^2 &\equiv \frac{1}{m}\iint_A \rho\eta^2 \, d\eta d\xi \quad & k_{m_2}^2 &\equiv \frac{1}{m}\iint_A \rho\xi^2 \, d\eta d\xi \\
k_m^2 &\equiv k_{m_1}^2 + k_{m_2}^2
\end{aligned}
$$

Stress Resultant-Displacement Equations

The strain-displacement equations are identical to those found in Ref 2:

$$
\begin{aligned}
\epsilon_{xx} &= u' + \frac{v'^2}{2} + \frac{w'^2}{2} - \lambda\phi'' \\
&\quad - v''\left[\eta\cos(\theta+\phi) - \xi\sin(\theta+\phi)\right] \\
&\quad - w''\left[\eta\cos(\theta+\phi) - \xi\sin(\theta+\phi)\right] \\
&\quad + (\eta^2 + \xi^2)\left(\theta'\phi' + \frac{\phi'^2}{2}\right) \\
\epsilon_{x\eta} &= -(\xi + \lambda_\eta)\phi' \qquad (9) \\
\epsilon_{x\xi} &= (\eta + \lambda_\xi)\phi'
\end{aligned}
$$

It is assumed that $\sigma_{\eta\eta} = \sigma_{\eta\xi} = \sigma_{\xi\xi} = 0$. Now, using Equations (9) and Hooke's Law, the axial force on the blade can be expressed as

$$
\begin{aligned}
V_{x'} &= \iint_A \sigma_{xx}\,d\eta d\xi = \iint_A E\epsilon_{xx}\,d\eta d\xi \qquad (10) \\
&= EA\left(u' + \frac{v'^2}{2} + \frac{w'^2}{2} + k_A^2\theta'\phi'\right. \\
&\quad \left. - e_A\left[v''\cos(\theta+\phi) + w''\sin(\theta+\phi)\right]\right)
\end{aligned}
$$

The resultant moments are

$$M_{x'} = \frac{\partial}{\partial x} \iint_A \lambda \sigma_{xx} d\eta d\xi + \iint_A \left[\eta \sigma_{x\xi} - \xi \sigma_{x\eta} \right.$$

$$\left. + \lambda \left(\frac{\partial \sigma_{x\eta}}{\partial \eta} + \frac{\partial \sigma_{x\xi}}{\partial \xi} \right) \right] d\eta d\xi \qquad (11)$$

$$= \left(GJ + EB_1 \theta' \right) \phi' + EA k_A^2 (\theta' + \phi') \times$$

$$\left(u' + \frac{v'^2}{2} + \frac{w'^2}{2} \right) - EB_2 \theta' \times$$

$$\left(v'' \cos \theta + w'' \sin \theta \right)$$

$$- \left[EC_1 \phi'' + EC_1^* (w'' \cos \theta - v'' \sin \theta) \right]'$$

$$M_{y'} = \iint_A \xi \sigma_{xx} d\eta d\xi \qquad (12)$$

$$= EI_{y'} \left[v'' \sin(\theta + \phi) - w'' \cos(\theta + \phi) \right]$$

$$M_{z'} = - \iint_A \eta \sigma_{xx} d\eta d\xi \qquad (13)$$

$$= EI_{z'} \left[v'' \cos(\theta + \phi) + w'' \sin(\theta + \phi) \right]$$

$$- EA e_A \left(u' + \frac{v'^2}{2} + \frac{w'^2}{2} \right) - EB_2 \theta' \phi'$$

where the blade geometrical constants are defined as

$$A \equiv \iint_A d\eta d\xi \qquad e_A \equiv \frac{1}{A} \iint_A \eta d\eta d\xi$$

$$k_A^2 \equiv \frac{1}{A} \iint_A \eta^2 + \xi^2 d\eta d\xi \qquad I_{y'} \equiv \iint_A \xi^2 d\eta d\xi$$

$$J \equiv \iint_A \hat{\eta}^2 + \hat{\xi}^2 d\eta d\xi \qquad I_{z'} \equiv \iint_A \eta^2 d\eta d\xi$$

$$B_1 \equiv \iint_A \left(\eta^2 + \xi^2 \right)^2 d\eta d\xi \qquad C_1 \equiv \iint_A \lambda^2 d\eta d\xi$$

$$B_2 \equiv \iint_A \eta \left(\eta^2 + \xi^2 \right) d\eta d\xi \qquad C_1^* \equiv \iint_A \xi \lambda d\eta d\xi$$

and the remaining integrals not included are negligible or identically equal to zero, due to the antisymmetry of the warping function, λ, and the assumed symmetry of the blade cross-section.

Substituting Equations (7), (8), (11), (12), and (13) into Equations (4-5), and Equations (7) and (10) into (6) the final four equations of motion are derived. Due to the length of these final equations, they are included in Appendix B.

Cantilever Blade Boundary Conditions   The helicopter blade rigidly attached to the hub has identical boundary conditions to a cantilever beam. These can be expressed as

$$u = v = v' = w = w' = \phi = 0$$

$$\{ x = 0 \}$$

and

$$M_{x'} = M_{y'} = M_{z'} = V_{x'} = V_y = V_z = 0$$

$$\{ x = R \}$$

Using the expressions for the shear forces in terms of stress resultants, i.e.,

$$V_y = -M'_{y'} \sin(\theta + \phi) - M'_{z'} \cos(\theta + \phi) - q_z$$

$$V_z = M'_{y'} \cos(\theta + \phi) - M'_{z'} \sin(\theta + \phi) + q_y$$

the shear force boundary conditions at $x = R$ can be rewritten as

$$-M'_{y'} \sin(\theta + \phi) - M'_{z'} \cos(\theta + \phi) - q_z = 0$$

$$M'_{y'} \cos(\theta + \phi) - M'_{z'} \sin(\theta + \phi) + q_y = 0$$

Numerical Solution for Cantilever Case

The cantilever blade can be analyzed as a special case of the presented formulation. To this end, the length of the links are set equal to zero, also the hinges are inactivated by setting the hinge angles equal to zero. To solve the resulting system of the equations of motion they were transformed into the state space representation. These equations were then transformed into a set of finite difference equations using the following central difference scheme for initial-boundary value problems (Ref 12).

$$\lambda\left(x + \frac{\Delta x}{2}, t + \frac{\Delta t}{2} \right) = \frac{1}{4} \left[\lambda_{i+1}^{j+1} + \lambda_{i+1}^{j} + \lambda_i^{j+1} + \lambda_i^{j} \right]$$

$$\frac{\partial \lambda}{\partial t}\left(x + \frac{\Delta x}{2}, t + \frac{\Delta t}{2} \right) = \frac{1}{2\Delta t} \left[\lambda_{i+1}^{j+1} - \lambda_{i+1}^{j} + \lambda_i^{j+1} - \lambda_i^{j} \right]$$

$$\frac{\partial \lambda}{\partial x}\left(x + \frac{\Delta x}{2}, t + \frac{\Delta t}{2} \right) = \frac{1}{2\Delta x} \left[\lambda_{i+1}^{j+1} + \lambda_{i+1}^{j} - \lambda_i^{j+1} - \lambda_i^{j} \right]$$

with second order accuracy, $O(\Delta x^2, \Delta t^2)$, and where λ refers to a general state space variable.

A numerical solution algorithm in time and space similar to that used in Ref 12 has been applied. The numerical solution based on the mentioned formulation was applied for a NACA0012 airfoil 1.1 m in length, with an aluminium structural shell. The airfoil was modelled as a shell, with a chord length of 7.53 cm and a skin thickness of 1.5 mm. For the numerical values used in the simulation, and a graphical representation
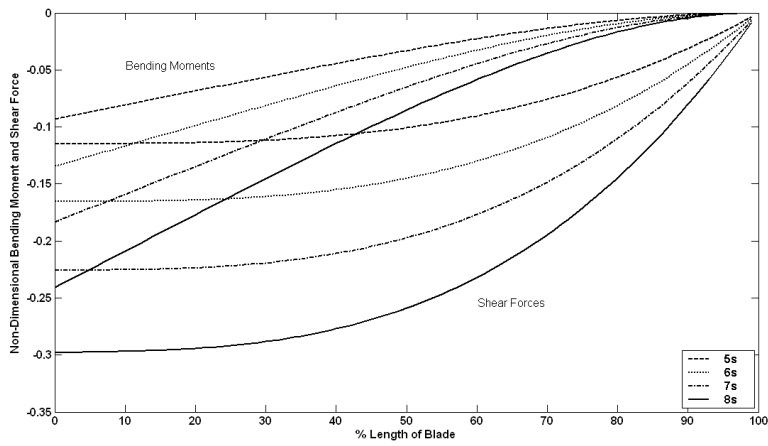
Figure 3: Lag bending moment and shear force diagram over 4 s at 1 s intervals
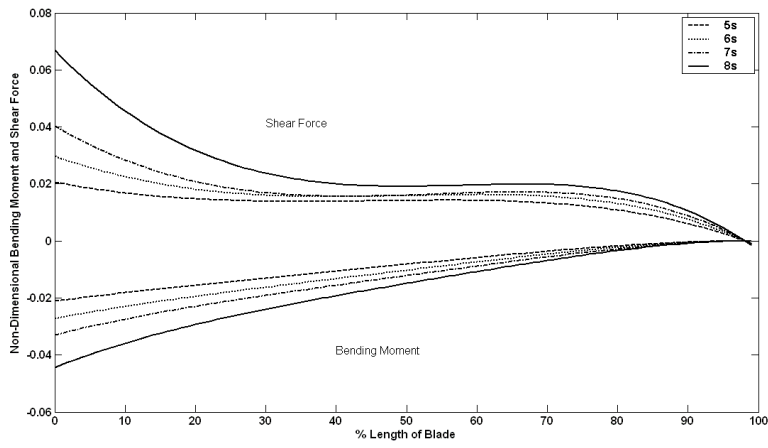

Figure 4: Flap bending moment and shear force diagram over 4 s at 1 s intervals
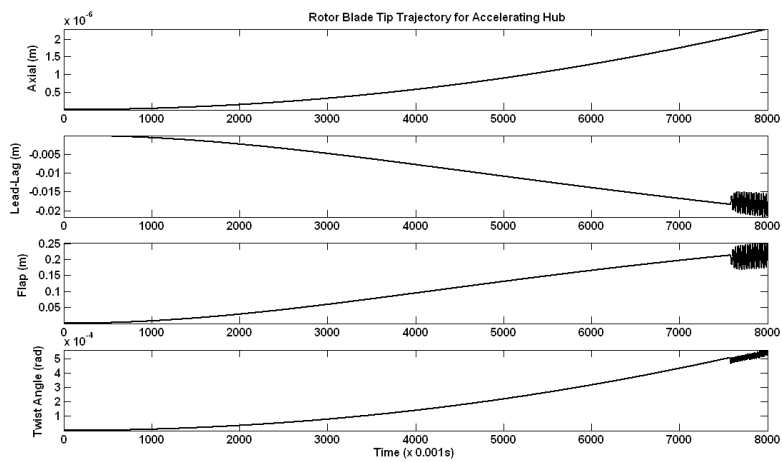

Figure 5: Tip trajectory from rest to 8 s of start-up phase

of the blade cross-section, see Fig C-1 in Appendix C.

The simulation was performed on a blade rigidly attached to the axis of rotation that emulated a rotating cantilever beam. The numerical experiment was conducted through a 10 s start-up phase, in which the rotor assembly underwent a constant angular acceleration of 20.6 rad/s^2, followed by a 5 s constant rotational velocity phase. The hover flight simulation results were obtained by applying basic aerodynamic excitations, see Ref 4, not including blade-vortex interactions.

Simulations were run to determine the sensitivity and stability of the results with respect to space and time step sizes. The blade was discretized into 99 elements and the simulation was run with a time step of 0.001 s.

The bending moment and shear force diagrams for the lead-lag and flap modes of motion of the cantilever blade are shown in Fig 3 and Fig 4, respectively. These figures show the bending moment and shear force at one second intervals beginning at 50% of the start-up speed. The bending moment and shear force have been non-dimensionalized by dividing the respective expressions by $m\Omega^2 R^2$ and $m\Omega^2 R$.

There are two observations that can be used to validate these results. First, the derivative of each bending moment roughly corresponds to the appropriate shear force, even though the shear forces were not calculated in that way. Second, the magnitudes of all of these stress resultants increase as the rotational velocity of the blade increases. This is expected since both the inertial and aerodynamic loads increase as the blade rotates more rapidly.

The time history diagrams of the tip deflection of the blade in different modes and for the first 8 s have been illustrated in Fig 5. At approximately 7.6 s into the simulation, an instability is observable. Higher order finite difference schemes are being applied in order to resolve this numerical issue.

Articulated Blade Boundary Conditions   In the articulated case, it is assumed that there is a plate attached to the inboard tip of the blade

that provides sufficient warping restraint. At this same position, there are two groups of constraints: the boundary conditions of the blade and the kinematic constraints of the linkage mechanism. Referring to the geometry of the links (Fig 2), the natural boundary conditions at this end are

$$T_{bl_o} = F_{ss_z}(d\cos\theta - (L + P_o)\sin\zeta)$$
$$- F_{ss_y}(d\sin\theta - (L + P_o)\sin\zeta\sin\beta)$$
$$- (L + P_o + P_i)\sin\zeta\,(V_z + V_y\sin\beta)$$

$$M_y = F_{ss_z}(F + (L + P_o))\cos\zeta$$
$$- F_{ss_x}(d\sin\theta - \sin\beta)$$
$$+ (F + (L + P_o + P_i)\cos\zeta)\,(V_z + V_x\sin\beta)$$

$$M_z = - F_{ss_y}(L + P_o)$$
$$- F_{ss_x}(d\cos\theta - (L + P_o)\sin\zeta)$$
$$- (V_y - V_x\sin\zeta)(L + P_o + P_i)$$

The remaining boundary conditions at this end are as follows

$$u = 0$$
$$\phi' = 0$$
$$v_{bl} = (L + P)\sin\zeta + v$$
$$w_{bl} = (F + (L + P)\cos\zeta)\sin\beta + w$$

where v and w refer to the blade elastic deformations in the blade co-ordinate system; and the total displacements, v_{bl} and w_{bl}, refer to the sum of the elastic deflections and the rigid body displacements. The boundary conditions at the outboard end are identical to those at the free end of the clamped blade.

Additionally, there is the following kinematic constraint equation arising from the coupling between the pitch bearing and the flap hinge:

$$\phi_0 = \frac{d\cos\theta\cos\zeta + (L + P_i)\sin\zeta}{(F + (L + P_i)\cos\beta)\cos\zeta - d(\cos\theta\sin\zeta + \sin\beta\sin\theta)}\beta$$

There is also coupling between pitch and lag that can be described as

$$\phi_0 = - \frac{d\sin\theta}{(L + P_i)\cos\zeta - d\cos\theta\sin\zeta}\zeta$$

Application of Impedance Control

An impedance controller for vibration attenuation of a system subjected to base-excitation has been illustrated in Ref 10.

In what follows, the same idea is utilized in a helicopter blade to reduce the motion of the controlled mass, i.e. the swash plate. The impedance control device is mounted on the swash plate and connects to the helicopter blade via the pitch horn (Fig 6).
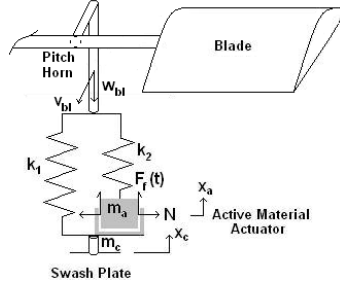

Figure 6: Impedance control device replacing the pitch link

To reduce the velocity of the controlled mass, its kinetic energy or linear momentum should be reduced. Both of these aims can be achieved by imposing controlled frictional damping.

Referring to Fig 6, the equations of motion of the impedance controller can be derived from Hamilton's principle:

$$\int_{t_1}^{t_2} [\delta(U - T) - \delta W]dt = 0$$

The kinetic and potential energies of the system are as follows

$$T = \frac{1}{2}m_a\dot{x}_a^2 + \frac{1}{2}m_c\dot{x}_c^2 + \frac{1}{2}\int_{Vol} \rho\vec{v}\cdot\vec{v}d\eta d\xi dx$$

$$U = \frac{1}{2}k_1(x_c - w_{bl})^2 + \frac{1}{2}k_2(x_a - w_{bl})^2$$
$$+ \frac{1}{2}\int_{Vol}(\sigma_{xx}\epsilon_{xx} + \sigma_{x\eta}\epsilon_{x\eta} + \sigma_{x\xi}\epsilon_{x\xi})d\eta d\xi dx$$

The final equations of motion of the impedance control device in the flap direction are

$$m_a\ddot{x}_a + k_2 x_a - k_2 w_{bl} = -F_f(t)$$
$$m_c\ddot{x}_c - k_1 w_{bl} + k_1 x_c = F_f(t) \qquad (14)$$

They should be supplemented by the corresponding equations in the other degrees of freedom and also the equations of motions of the blade itself.

The impedance control device utilizes piezoceramic actuators that can supply enough force to prevent slip between contact surfaces. In this way, they switch the system state between the 'uncoupled' three-body motion and 'coupled' two-body motion. Kinetic energy that would have been returned to the system in a reactive manner can be removed.

As demonstrated in Ref 10, the only information required to control the system is the absolute velocity of the controlled structure $(\dot{x}_c)$, and the relative velocity of the actuators to the controlled structure, $(\dot{x}_a - \dot{x}_c)$. The control algorithm will be an on/off switch that is based on the sign of the product of the preceding two terms.

$$C = \dot{x}_c (\dot{x}_a - \dot{x}_c) \qquad (15)$$

When C is negative, the actuating mass and swash plate are moving in opposite directions, so if the actuator is engaged it will reduce the motion of the controlled mass. Conversely, if C is positive, then the masses are moving in the same direction, and the actuator should be disengaged to prevent amplification of the motion of the controlled mass. This idea of 'state-switching' was proposed in Ref 13.

The simulink model of the state-switch controller is shown in Ref 10. This controller would be used in conjunction with a MATLAB code in order to determine the elastic deflections and rigid body motions of the blade.

Conclusions

In this paper, the non-linear behaviour of an articulated rotorcraft blade with and without a control device was formulated. The formulation included bending (in both lead-lag and flap), together with torsion and extensional equations of motion for an articulated rotorcraft blade. It also described the articulated blade boundary constraints where the pitch link was replaced by an impedance control device. The impedance control device was modelled, and an algorithm for the reduction of the transmissibility ratio was presented. The set of equations of motion for the non-articulated blade and its boundary conditions were solved using a finite difference scheme. Having obtained the numerical results, the dynamic bending moment and shear force diagrams for the cantilever blade were illustrated. The tip trajectories were also plotted, and a more accurate finite difference scheme was determined to be necessary for convergence.

References

[1] Houbolt, J.C. and Brooks, G.W., *Differential Equations of Motion for Combined Flapwise Bending, Chordwise Bending, and Torsion of Twisted Nonuniform Rotor Blades,* (Washington DC., USA: NASA Report 1346, 1958).

[2] Hodges, D.H. and Dowell, E.H., *Nonlinear Equations of Motion for the Elastic Bending and Torsion of Twisted Nonuniform Rotor Blades,* (Washington DC., USA: NASA TN D-7818, December, 1974).

[3] Bramwell, A.R.S., *Helicopter Dynamics*, (London, UK: Edward Arnold 1976).

[4] Hodges, D.H. and Ormiston, R.A., *Stability of Elasticy Bending and Torsion of Uniform Cantilever Rotor blades in Hover with Variable Structural Coupling,* (Washington DC., USA: NASA TN D-8192, April, 1976).

[5] Johnson, *Helicopter Dynamics* (Princeton, New Jersey, USA: Princeton University Press 1980).

[6] Zheng, Z.C., Ren, G., and Cheng, Y.M., "Aeroelastic Responce of a Couple Rotor/Fuselage System in Hovering and Forward Flight", *Archive of Applied Mechanics* **Vol. 69**, 1999, pp. 68-82.

[7] Al-Bedoor, B.O., "Dynamic Model of Coupled Shaft Torsional and Blade Bending Deformations in Rotors", *Computer Methods in Applied Mechanics and Engineering,***Vol. 169**, 1999, pp. 177-190.

[8] Cesnik, C.E.S., Opoku, D.G., Nitzsche, F., and Cheng, T., "Active Twist Rotor Blade Modelling using Particle-Wake Aerodynamics and Geometrically Exact Beam Structural Dynamics", *Journal of Fluids and Structures,* **Vol. 19**, 2004. pp. 651-668.

[9] Nitzsche, F., *Smart-Spring Actuation for Helicopter Individual Blade Control,* (Sixth International Conference on Adaptive Structures, Technomic, Lancaster-Basel, 1996), pp. 230-240.

[10] Harold, Tim, *Performance Characterization of the Smart Spring Concept for Indirect-Active Vibration Suppression,* (Ottawa, Canada: Carleton University Master of Applied Science Thesis, 2004).

[11] Niku, Saeed, *Introduction to Robotics: Analysis, Systems, Applications* (San Luis Obispo, California, USA: Prentice Hall, 2001).

[12] Esmailzadeh, E., and Ghorashi, M., "Vibration analysis of a Timoshenko Beam Subjected to a Travelling Mass," *Journal of Sound and Vibration* **Vol. 199**(4), 1997, pp. 615-628.

[13] Cunefare, K.A., "State-Switched Absorber for Vibration Control of Point-Excited Beams," *Journal of Intelligent Material Systems and Structures,* **Vol. 13**(2), February 2002, pp. 97-105.

APPENDIX A

The transformation matrix below describes the position and orientation of the helicopter blade with respect to the inertial frame of reference attached to the hub.

$$T_6 = \begin{bmatrix} \cos\psi\cos\beta\cos\zeta & -\cos\psi\cos\beta\sin\zeta & -\cos\psi\sin\beta & (\cos\psi\cos\beta\cos\zeta - \sin\psi\sin\zeta)(P+L) \\ -\sin\psi\sin\zeta & -\sin\psi\cos\zeta & & +\cos\psi\cos\beta F + \cos\psi E* \\ \\ \sin\psi\cos\beta\cos\zeta & -\sin\psi\cos\beta\sin\zeta & -\sin\psi\sin\beta & (\sin\psi\cos\beta\cos\zeta + \cos\psi\sin\zeta)(P+L) \\ +\cos\psi\sin\zeta & +\cos\psi\cos\zeta & & +\sin\psi\cos\beta F + \sin\psi E* \\ \\ \sin\beta\cos\zeta & -\sin\beta\sin\zeta & \cos\beta & \sin\beta\cos\zeta(P+L) + \sin\beta F \\ \\ 0 & 0 & 0 & 1 \end{bmatrix} \quad \text{(A-1)}$$

APPENDIX B

The following equations of motion describe the dynamics of the articulated helicopter blade with respect to the inertial co-ordinate frame. However, the integrals and derivatives are properly taken with respect to the rotor blade co-ordinate frame. The aerodynamic terms are left unknown, however, the aerodynamic loading, according to Ref 4, was used to solve for the hover flight condition.

The δu equation (longitudinal extension) is:

$$EA\left\{ u' + \frac{v'^2}{2} + \frac{w'^2}{2} + k_A^2\theta'\phi' - e_A\left[v''\cos(\theta+\phi) + w''\sin(\theta+\phi)\right] \right\}' = T' =$$

$$-m\left\{ \sin\psi\,\ddot{v} + 2\left(\cos\psi\dot{\zeta} + \cos\psi\dot{\psi}\right)\dot{v} + 2\cos\psi\dot{\beta}\,\dot{w} + \left(\cos\psi\dot{\psi}^2 - 2\sin\psi\dot{\psi}\beta\dot{\beta} + \cos\psi\ddot{\psi}\zeta\right. \right.$$

$$+ \sin\psi\ddot{\psi} - 2\sin\psi\dot{\psi}\zeta\dot{\zeta} + \cos\psi\dot{\beta}^2 + \cos\psi\beta\ddot{\beta} + \sin\psi\ddot{\zeta} + \cos\psi\dot{\zeta}^2 + \cos\psi\zeta\ddot{\zeta} - \sin\psi\dot{\psi}^2\zeta$$

$$\left. + 2\cos\psi\dot{\psi}\dot{\zeta} - \sin\psi\zeta\dot{\zeta}^2\right)x + \left(\cos\psi\ddot{\zeta} - 2\sin\psi\dot{\psi}\dot{\zeta} - \sin\psi\dot{\psi}^2 - \sin\psi\dot{\zeta}^2 + \cos\psi\ddot{\psi}\right) \times$$

$$(v + e\cos\theta) - \left(2\sin\psi\dot{\psi}\dot{\beta} - \cos\psi\ddot{\beta}\right)(w + e\sin\theta)$$

$$+ \left(\cos\psi\dot{\psi}^2 + \cos\psi\dot{\beta}^2 + \cos\psi\dot{\zeta}^2 + 2\cos\psi\dot{\psi}\dot{\zeta} + \sin\psi\ddot{\zeta} + \sin\psi\ddot{\psi}\right)(P+L)$$

$$+ \left(\cos\psi\dot\psi^2 + \cos\psi\dot\beta^2 + \sin\psi\ddot\psi \right) F + \left(\cos\psi\dot\psi^2 + \sin\psi\ddot\psi \right) E* - \left(\sin\psi\dot\psi^2 + 2\cos\psi\dot\psi\beta\dot\beta \right.$$

$$+ 2\cos\psi\dot\psi\zeta\dot\zeta + \sin\psi\dot\beta^2 + \sin\psi\beta\ddot\beta - 2\sin\psi\beta\dot\beta\zeta\dot\zeta + \sin\psi\dot\zeta^2 + \sin\psi\zeta\ddot\zeta + \cos\psi\dot\psi^2\zeta + \sin\psi\ddot\psi\zeta$$

$$\left. +2\sin\psi\dot\psi\dot\zeta + \cos\psi\zeta\dot\zeta^2 - \cos\psi\zeta\ddot\zeta - \cos\psi\ddot\psi \right) \left(\frac{1}{2}v''(R^2 - x^2) - v'x \right)$$

$$\left. - \left(\beta\dot\beta^2 - \ddot\beta + 2\dot\beta\dot\zeta + \beta\dot\zeta^2 + \beta\zeta\ddot\zeta \right) \left(\frac{1}{2}w''(R^2 - x^2) - w'x \right) \right\} \tag{B-1}$$

The δv equation (lead-lag bending) is:

$$L_v = \left[\left(EI_{y'} \left[v'' \sin(\theta + \phi) - w'' \cos(\theta + \phi) \right] - EC_1^*\phi'' \right) \sin(\theta + \phi) + \cos(\theta + \phi) \times \right.$$

$$\left(-EAe_A \left(u' + \frac{v'^2}{2} + \frac{w'^2}{2} \right) - EB_2^*\theta'\phi' + EI_{z'} \left[v'' \cos(\theta + \phi) + w'' \sin(\theta + \phi) \right] \right) \right]''$$

$$- m \left(v' \int_x^R \left\{ \sin\psi \, \ddot v + 2 \left(\cos\psi\dot\zeta + \cos\psi\dot\psi \right) \dot v + 2\cos\psi\dot\beta \, \dot w + \left(\cos\psi\dot\psi^2 + \sin\psi\ddot\zeta \right) \right. \right.$$

$$- 2\sin\psi\dot\psi\zeta\dot\zeta + \cos\psi\dot\beta^2 + \cos\psi\dot\zeta^2 - 2\sin\psi\dot\psi\beta\dot\beta + \cos\psi\zeta\ddot\zeta - \sin\psi\dot\psi^2\zeta + \sin\psi\ddot\psi$$

$$+ \cos\psi\ddot\psi\zeta + \cos\psi\beta\ddot\beta + 2\cos\psi\dot\psi\dot\zeta - \sin\psi\zeta\dot\zeta^2 \right) x + \left(\cos\psi\ddot\zeta - 2\sin\psi\dot\psi\dot\zeta - \sin\psi\dot\psi^2 \right.$$

$$\left. - \sin\psi\dot\zeta^2 + \cos\psi\ddot\psi \right) (v + e\cos\theta) - \left(2\sin\psi\dot\psi\dot\beta - \cos\psi\ddot\beta \right) (w + e\sin\theta)$$

$$+ \left(\cos\psi\dot\psi^2 + \cos\psi\dot\beta^2 + \cos\psi\dot\zeta^2 + 2\cos\psi\dot\psi\dot\zeta + \sin\psi\ddot\zeta + \sin\psi\ddot\psi \right) (P + L)$$

$$\left. + \left(\cos\psi\dot\psi^2 + \cos\psi\dot\beta^2 + \sin\psi\ddot\psi \right) F + \left(\cos\psi\dot\psi^2 + \sin\psi\ddot\psi \right) E* \right\} dx \right)'$$

$$+ m \left\{ \sin\psi \left(\ddot u - e(\ddot v' \cos\theta + \ddot w' \sin\theta) \right) - \sin\psi\zeta\ddot v + \cos\psi \left(\ddot v - e\ddot\phi\sin\theta \right) \right.$$

$$+ 2 \left(\cos\psi\dot\psi + \cos\psi\dot\zeta \right) \left(\dot u - e(\dot v'\cos\theta + \dot w'\sin\theta) \right) - 2 \left(\sin\psi\dot\psi + \sin\psi\dot\zeta \right) \times$$

$$\left(\dot v - e\dot\phi\sin\theta \right) - 2 \left(\cos\psi\dot\psi\zeta + \cos\psi\zeta\dot\zeta \right) \dot v - 2\sin\psi\dot\beta \left(\dot w + e\dot\phi\cos\theta \right)$$

$$- 2\cos\psi\dot\psi\beta \, \dot w - \left(\sin\psi\dot\psi^2 + \sin\psi\dot\beta^2 + \sin\psi\dot\zeta^2 + 2\sin\psi\dot\psi\dot\zeta - \cos\psi\ddot\zeta - \cos\psi\ddot\psi \right)$$

$$\times \left(u - e(v'\cos\theta + w'\sin\theta) \right) - \ddot w \sin\psi\beta$$

$$- \left(\sin\psi\dot\psi^2 + 2\cos\psi\dot\psi\beta\dot\beta + 2\cos\psi\dot\psi\zeta\dot\zeta + \sin\psi\dot\beta^2 + \sin\psi\beta\ddot\beta - 2\sin\psi\beta\dot\beta\zeta\dot\zeta - \cos\psi\ddot\psi \right.$$

$$\left. + \sin\psi\dot\zeta^2 + \sin\psi\zeta\ddot\zeta + \cos\psi\dot\psi^2\zeta + 2\sin\psi\dot\psi\dot\zeta + \cos\psi\zeta\dot\zeta^2 - \cos\psi\zeta\ddot\zeta + \sin\psi\ddot\psi\zeta \right) x$$

$$- \left(2\cos\psi\dot\psi\dot\zeta + \sin\psi\ddot\zeta + \cos\psi\dot\psi^2 + \cos\psi\dot\zeta^2 + \sin\psi\ddot\psi \right) (v + e\cos(\theta + \phi))$$

$$+ \left(\sin\psi\dot\psi^2\zeta - \cos\psi\ddot\psi\zeta + \sin\psi\dot\beta^2\zeta + 2\sin\psi\beta\dot\beta\dot\zeta + \sin\psi\zeta\dot\zeta^2 + 2\sin\psi\dot\psi\zeta\dot\zeta - \cos\psi\zeta\ddot\zeta \right)$$

$$\times (v + e\cos\theta) - \left(2\cos\psi\dot\psi\dot\beta + \sin\psi\ddot\beta \right) (w + e\sin(\theta + \phi))$$

$$+ \left(\sin\psi\dot\psi^2\beta + \sin\psi\beta\dot\beta^2 \right) (w + e\sin\theta)$$

$$- \left(\sin\psi\dot\psi^2 + 2\cos\psi\dot\psi\beta\dot\beta + 2\cos\psi\dot\psi\zeta\dot\zeta + \sin\psi\dot\beta^2 + \sin\psi\beta\ddot\beta + \sin\psi\dot\zeta^2 - \cos\psi\ddot\psi \right.$$

$$\left. + \sin\psi\zeta\ddot\zeta + \cos\psi\dot\psi^2\zeta + 2\sin\psi\dot\psi\dot\zeta + \cos\psi\zeta\dot\zeta^2 - \cos\psi\zeta\ddot\zeta + \sin\psi\ddot\psi\zeta \right) (P + L)$$

$$\left. - \left(\sin\psi\dot\psi^2 + 2\cos\psi\dot\psi\beta\dot\beta + \sin\psi\dot\beta^2 + \sin\psi\beta\ddot\beta - \cos\psi\ddot\psi \right) F - \left(\sin\psi\dot\psi^2 - \cos\psi\ddot\psi \right) E* \right\}$$

$$+ m \left\{ e\cos\theta \left[-\sin\psi\ddot v - 2 \left(\cos\psi\dot\zeta + \cos\psi\dot\psi \right) \dot v - 2\cos\psi\dot\beta\dot w + \right. \right.$$

$$\left(2\sin\psi\beta\dot\beta + 2\sin\psi\dot\psi\zeta\dot\zeta - \cos\psi\beta\ddot\beta - \cos\psi\zeta\ddot\zeta + \sin\psi\dot\psi^2\zeta + \sin\psi\,\zeta\dot\zeta^2 - \cos\psi\ddot\psi\zeta \right) x$$

$$- \left(\cos\psi\ddot\zeta - 2\sin\psi\dot\psi\dot\zeta - \sin\psi\dot\psi^2 - \sin\psi\dot\zeta^2 + \cos\psi\ddot\psi \right) v + \left(2\sin\psi\dot\psi\dot\beta - \cos\psi\ddot\beta \right) w$$

$$- \left(\sin\psi\ddot\zeta + \cos\psi\dot\psi^2 + \cos\psi\dot\beta^2 + \cos\psi\dot\zeta^2 + 2\cos\psi\dot\psi\dot\zeta + \sin\psi\ddot\psi \right) (P + L)$$

$$\left. - \left(\cos\psi\dot\psi^2 + \cos\psi\dot\beta^2 + \sin\psi\ddot\psi \right) F - \left(\cos\psi\dot\psi^2 + \sin\psi\ddot\psi \right) E* \right]$$

$$\left. - e\cos(\theta + \phi) \left[\left(\cos\psi\dot\psi^2 + \sin\psi\ddot\psi + \cos\psi\dot\beta^2 + \cos\psi\dot\zeta^2 + \sin\psi\ddot\zeta + 2\cos\psi\dot\psi\dot\zeta \right) x \right] \right.$$

$$+ \left(k_{m_2}^2 - k_{m_1}^2\right) \cos\theta \sin\theta \left[2\sin\psi\dot{\psi}\dot{\beta} - \cos\psi\ddot{\beta}\right]$$

$$+ \left(k_{m_2}^2 \cos^2\theta + k_{m_1}^2 \sin^2\theta\right) \left[-\cos\psi\ddot{\zeta} + 2\sin\psi\dot{\psi}\dot{\zeta} + \sin\psi\dot{\psi}^2 + \sin\psi\dot{\zeta}^2 - \cos\psi\ddot{\psi}\right]\Bigg\}' \tag{B-2}$$

The δw equation (flap bending) is:

$$L_w = \Bigg[\left(EI_{y'}\left[v''\sin(\theta+\phi) - w''\cos(\theta+\phi)\right] - EC_1^*\phi''\right)\cos(\theta+\phi) - \sin(\theta+\phi)\times$$

$$\left(-EAe_A\left(u' + \frac{v'^2}{2} + \frac{w'^2}{2}\right) - EB_2^*\theta'\phi' + EI_{z'}\left[v''\cos(\theta+\phi) + w''\sin(\theta+\phi)\right]\right)\Bigg]''$$

$$+ m\left(w'\int_x^R \left\{\sin\psi\,\ddot{v} + 2\left(\cos\psi\dot{\zeta} + \cos\psi\dot{\psi}\right)\dot{v} + 2\cos\psi\dot{\beta}\dot{w} + \left(\cos\psi\dot{\psi}^2 + \sin\psi\ddot{\zeta}\right.\right.\right.$$

$$- 2\sin\psi\dot{\psi}\zeta\dot{\zeta} + \cos\psi\dot{\beta}^2 + \cos\psi\dot{\zeta}^2 - 2\sin\psi\dot{\psi}\beta\dot{\beta} + \cos\psi\zeta\ddot{\zeta} - \sin\psi\dot{\psi}^2\zeta + \cos\psi\ddot{\psi}\zeta$$

$$+ \cos\psi\beta\ddot{\beta} + 2\cos\psi\dot{\psi}\dot{\zeta} - \sin\psi\zeta\dot{\zeta}^2 + \sin\psi\ddot{\psi}\big)x + \left(\cos\psi\ddot{\zeta} - 2\sin\psi\dot{\psi}\dot{\zeta} - \sin\psi\dot{\psi}^2\right.$$

$$- \sin\psi\dot{\zeta}^2 + \cos\psi\ddot{\psi}\big)(v + e\cos\theta) - \left(2\sin\psi\dot{\psi}\dot{\beta} - \cos\psi\ddot{\beta}\right)(w + e\sin\theta)$$

$$+ \left(\cos\psi\dot{\psi}^2 + \cos\psi\dot{\beta}^2 + \cos\psi\dot{\zeta}^2 + 2\cos\psi\dot{\psi}\dot{\zeta} + \sin\psi\ddot{\zeta} + \sin\psi\ddot{\psi}\right)(P+L)$$

$$+ \left(\cos\psi\dot{\psi}^2 + \cos\psi\dot{\beta}^2 + \sin\psi\ddot{\psi}\right)F + \left(\cos\psi\dot{\psi}^2 + \sin\psi\ddot{\psi}\right)E*\bigg\}\,dx\right)'$$

$$- m\left\{\ddot{w} + e\ddot{\phi}\cos\theta + 2\dot{\beta}\left(\dot{u} - e(\dot{v}'\cos\theta + \dot{w}'\sin\theta)\right) - 2\left(\dot{\beta}\zeta + \beta\dot{\zeta}\right)\dot{v} - 2\beta\dot{\beta}\dot{w}\right.$$

$$+ \ddot{\beta}(u - e(v'\cos\theta + w'\sin\theta)) + \left(-\beta\dot{\beta}^2 + \ddot{\beta} - 2\dot{\beta}\zeta\dot{\zeta} - \beta\dot{\zeta}^2 - \beta\zeta\ddot{\zeta}\right)x$$

$$- 2\dot{\beta}\dot{\zeta}(v + e\cos(\theta+\phi)) - \left(\ddot{\beta}\zeta + \beta\ddot{\zeta}\right)(v + e\cos\theta) - \dot{\beta}^2(w + e\sin(\theta+\phi))$$

$$- \beta\ddot{\beta}(w + e\sin\theta) + \left(\ddot{\beta} - \beta\dot{\beta}^2 - 2\dot{\beta}\zeta\dot{\zeta} - \beta\dot{\zeta}^2\right)(P+L) - \left(\beta\dot{\beta}^2 - \ddot{\beta}\right)F\right\}$$

$$- m\left\{e\sin\theta\left[-\sin\psi\ddot{v} - 2\left(\cos\psi\dot{\zeta} + \cos\psi\dot{\psi}\right)\dot{v} - 2\cos\psi\dot{\beta}\dot{w} + \right.\right.$$

$$\left(2\sin\psi\dot{\psi}\beta\dot{\beta} + 2\sin\psi\dot{\psi}\zeta\dot{\zeta} - \cos\psi\beta\ddot{\beta} - \cos\psi\zeta\ddot{\zeta} + \sin\psi\dot{\psi}^2\zeta + \sin\psi\,\zeta\dot{\zeta}^2 - \cos\psi\ddot{\psi}\zeta\right)x$$

$$- \left(\cos\psi\ddot{\zeta} - 2\sin\psi\dot{\psi}\dot{\zeta} - \sin\psi\dot{\psi}^2 - \sin\psi\dot{\zeta}^2 + \cos\psi\ddot{\psi}\right)v + \left(2\sin\psi\dot{\psi}\dot{\beta} - \cos\psi\ddot{\beta}\right)w$$

$$- \left(\sin\psi\ddot{\zeta} + \cos\psi\dot{\psi}^2 + \cos\psi\dot{\beta}^2 + \cos\psi\dot{\zeta}^2 + 2\cos\psi\dot{\psi}\dot{\zeta} + \sin\psi\ddot{\psi}\right)(P+L)$$

$$- \left(\cos\psi\dot{\psi}^2 + \cos\psi\dot{\beta}^2 + \sin\psi\ddot{\psi}\right)F - \left(\cos\psi\dot{\psi}^2 + \sin\psi\ddot{\psi}\right)E*\right]$$

$$- e\sin(\theta+\phi)\left[\left(\cos\psi\dot{\psi}^2 + \cos\psi\dot{\beta}^2 + \cos\psi\dot{\zeta}^2 + \sin\psi\ddot{\zeta} + 2\cos\psi\dot{\psi}\dot{\zeta} + \sin\psi\ddot{\psi}\right)x\right]$$

$$+ \left(k_{m_2}^2 - k_{m_1}^2\right)\cos\theta\sin\theta\left[-\cos\psi\ddot{\zeta} + 2\sin\psi\dot{\psi}\dot{\zeta} + \sin\psi\dot{\psi}^2 + \sin\psi\dot{\zeta}^2 - \cos\psi\ddot{\psi}\right]$$

$$+ \left(k_{m_2}^2 \sin^2\theta + k_{m_1}^2 \cos^2\theta\right)\left[2\sin\psi\dot{\psi}\dot{\beta} - \cos\psi\ddot{\beta}\right]\Bigg\}' \tag{B-3}$$

The $\delta\phi$ equation (aeroelastic twist) is:

$$M_\phi = \left(GJ\phi' + EAk_A^2(\theta+\phi)'\left(u' + \frac{v'^2}{2} + \frac{w'^2}{2}\right) + EB_1^*\theta'^2\phi'\right.$$

$$\left.- EB_2^*\theta'\left(v''\cos\theta + w''\sin\theta\right) - \left[EC_1\phi'' + EC_1^*\left(w''\cos\theta - v''\sin\theta\right)\right]'\right)' -$$

$$\left(EI_{y'}\left[v''\sin(\theta+\phi) - w''\cos(\theta+\phi)\right] - EC_1^*\phi''\right)\left[v''\cos(\theta+\phi) + w''\sin(\theta+\phi)\right]$$

$$+ \left(-EAe_A\left(u' + \frac{v'^2}{2} + \frac{w'^2}{2}\right) - EB_2^*\theta'\phi' + EI_{z'}\left[v''\cos(\theta+\phi) + w''\sin(\theta+\phi)\right]\right)$$

$$\times \left[v''\sin(\theta+\phi) - w''\cos(\theta+\phi)\right]$$

$$+ m\left\{e\sin\theta\left[\sin\psi\ddot{u} - \left(\sin\psi\dot{\psi}^2 + \sin\psi\dot{\beta}^2 + \sin\psi\dot{\zeta}^2 + 2\sin\psi\dot{\psi}\dot{\zeta} - \cos\psi\ddot{\zeta} - \cos\psi\ddot{\psi}\right)u\right.\right.$$

$$+ 2\left(\cos\psi\dot{\psi} + \cos\psi\dot{\zeta}\right)\dot{u} - \sin\psi\zeta\ddot{v} - 2\cos\psi\dot{\beta}\dot{w} - 2\left(\cos\psi\dot{\psi}\zeta + \cos\psi\zeta\dot{\zeta}\right)\dot{v}$$

$$+ 2\sin\psi\beta\dot{\beta}\zeta\dot{\zeta}x + \left(\sin\psi\dot{\psi}^2\zeta + \sin\psi\dot{\beta}^2\zeta + 2\sin\psi\beta\dot{\beta}\dot{\zeta} + \sin\psi\zeta\dot{\zeta}^2 + 2\sin\psi\dot{\psi}\zeta\dot{\zeta} - \cos\psi\ddot{\psi}\zeta\right.$$

$$\left.- \cos\psi\zeta\ddot{\zeta}\right)v - \ddot{w}\sin\psi\beta + \left(\sin\psi\dot{\psi}^2\beta + \sin\psi\beta\dot{\beta}^2\right)w - \left(2\cos\psi\dot{\psi}\beta\dot{\beta} + 2\cos\psi\dot{\psi}\zeta\dot{\zeta}\right.$$

$$+ \sin\psi\beta\ddot{\beta} + \sin\psi\zeta\ddot{\zeta} + \cos\psi\dot{\psi}^2\zeta + \cos\psi\zeta\dot{\zeta}^2 + \sin\psi\ddot{\psi}\zeta\big)(P+L) + \left(-\sin\psi\beta\ddot{\beta}\right.$$

$$-2\cos\psi\dot\psi\beta\dot\beta\Big)\,F\Big]+e\sin(\theta+\phi)\Big[\cos\psi\ddot v-2\sin\psi\dot\beta\dot w-2\left(\sin\psi\dot\psi+\sin\psi\dot\zeta\right)\dot v$$

$$-\left(\sin\psi\dot\psi^2+2\cos\psi\dot\psi\beta\dot\beta+2\cos\psi\dot\psi\zeta\dot\zeta+\sin\psi\dot\beta^2+\sin\psi\beta\ddot\beta+\sin\psi\ddot\psi\zeta-\cos\psi\ddot\psi\right.$$

$$\left.+\sin\psi\dot\zeta^2+\sin\psi\zeta\ddot\zeta+\cos\psi\dot\psi^2\zeta+2\sin\psi\dot\psi\dot\zeta+\cos\psi\zeta\dot\zeta^2-\cos\psi\ddot\zeta\right)x$$

$$-\left(2\cos\psi\dot\psi\dot\zeta+\sin\psi\ddot\zeta+\cos\psi\dot\psi^2+\cos\psi\dot\zeta^2+\sin\psi\ddot\psi\right)v-\left(2\cos\psi\dot\psi\dot\beta+\sin\psi\ddot\beta\right)w$$

$$-\left(\sin\psi\dot\psi^2+\sin\psi\dot\beta^2+\sin\psi\dot\zeta^2+2\sin\psi\dot\psi\dot\zeta-\cos\psi\ddot\zeta-\cos\psi\ddot\psi\right)(P+L)$$

$$+\left(\cos\psi\ddot\psi-\sin\psi\dot\psi^2-\sin\psi\dot\beta^2\right)F+\left(\cos\psi\ddot\psi-\sin\psi\dot\psi^2\right)E*\Big]$$

$$-e\cos\theta\,\Big[2\dot\beta\dot u+\ddot\beta u-2\left(\dot\beta\zeta+\beta\dot\zeta\right)\dot v-2\beta\dot\beta\dot w-\beta\zeta\ddot\zeta x$$

$$-\left(\ddot\beta\zeta+\beta\ddot\zeta\right)v+\beta\ddot\beta w-\left(\beta\dot\beta^2+2\dot\beta\zeta\dot\zeta+\beta\dot\zeta^2\right)(P+L)-\beta\dot\beta^2 F\Big]-e\cos(\theta+\phi)$$

$$\times\Big[\ddot w-\left(\beta\dot\beta^2-\ddot\beta+2\dot\zeta\dot\zeta+\beta\dot\zeta^2\right)x-2\dot\beta\dot\zeta v-\dot\beta^2 w+\ddot\beta(P+L)+\ddot\beta F\Big]$$

$$+(k_{m_2}^2-k_{m_1}^2)\cos\theta\sin\theta\Big[-\sin\psi\ddot v'-2\left(\cos\psi\dot\psi+\cos\psi\dot\zeta\right)\dot v'-2\sin\psi\dot\beta\dot\phi$$

$$+\sin\psi\dot\psi^2\zeta+\sin\psi\dot\beta^2\zeta+2\sin\psi\beta\dot\beta\dot\zeta+\sin\psi\zeta\dot\zeta^2+2\sin\psi\dot\psi\zeta\dot\zeta-\cos\psi\zeta\ddot\zeta-\cos\psi\ddot\psi\zeta$$

$$+2\dot\beta\dot w'+\beta\ddot\beta+w'\ddot\beta+v'\left(\sin\psi\dot\psi^2+\sin\psi\dot\beta^2+\sin\psi\dot\zeta^2+2\sin\psi\dot\psi\dot\zeta-\cos\psi\ddot\zeta-\cos\psi\ddot\psi\right)\Big]$$

$$+(k_{m_2}^2-k_{m_1}^2)\cos(\theta+\phi)\sin(\theta+\phi)\Big[\dot\beta^2-2\cos\psi\dot\psi\dot\zeta-\sin\psi\ddot\zeta-\sin\psi\ddot\psi$$

$$-\cos\psi\dot\psi^2-\cos\psi\dot\zeta^2\Big]+(k_{m_1}^2\cos^2\theta+k_{m_2}^2\sin^2\theta)\Big[-\sin\psi\ddot w'-\cos\psi\ddot\phi$$

$$-2\left(\cos\psi\dot\psi+\cos\psi\dot\zeta\right)\dot w'+2\left(\sin\psi\dot\psi+\sin\psi\dot\zeta\right)\dot\phi+\sin\psi\dot\psi^2\beta+\sin\psi\beta\dot\beta^2$$

$$+w'\left(\sin\psi\dot\psi^2+\sin\psi\dot\beta^2+\sin\psi\dot\zeta^2+2\sin\psi\dot\psi\dot\zeta-\cos\psi\ddot\zeta-\cos\psi\ddot\psi\right)\Big]$$

$$-(k_{m_1}^2\cos^2(\theta+\phi)+k_{m_2}^2\sin^2(\theta+\phi))\Big[2\cos\psi\dot\psi\dot\beta+\sin\psi\ddot\beta\Big]$$

$$-(k_{m_1}^2\sin^2\theta+k_{m_2}^2\cos^2\theta)\Big[\ddot\phi-2\dot\beta\dot v'-\ddot\beta\zeta-\beta\ddot\zeta-v'\ddot\beta\Big]$$

$$+(k_{m_1}^2\sin^2(\theta+\phi)+k_{m_2}^2\cos^2(\theta+\phi))\Big[2\dot\beta\dot\zeta\Big]\Big\}$$

$$-mv'\Big\{e\sin\theta\Big[-\sin\psi\ddot v-2\left(\cos\psi\dot\zeta+\cos\psi\dot\psi\right)\dot v-2\cos\psi\dot\beta\dot w$$

$$+\left(2\sin\psi\dot\psi\beta\dot\beta+2\sin\psi\dot\psi\zeta\dot\zeta-\cos\psi\beta\ddot\beta-\cos\psi\zeta\ddot\zeta+\sin\psi\dot\psi^2\zeta+\sin\psi\,\zeta\dot\zeta^2-\cos\psi\ddot\psi\zeta\right)x$$

$$-\left(\cos\psi\ddot\zeta-2\sin\psi\dot\psi\dot\zeta-\sin\psi\dot\psi^2-\sin\psi\dot\zeta^2+\cos\psi\ddot\psi\right)v+\left(2\sin\psi\dot\psi\dot\beta-\cos\psi\ddot\beta\right)w$$

$$-\left(\sin\psi\ddot\zeta+\cos\psi\dot\psi^2+\cos\psi\dot\beta^2+\cos\psi\dot\zeta^2+2\cos\psi\dot\psi\dot\zeta+\sin\psi\ddot\psi\right)(P+L)$$

$$-\left(\cos\psi\dot\psi^2+\cos\psi\dot\beta^2+\sin\psi\ddot\psi\right)F-\left(\cos\psi\dot\psi^2+\sin\psi\ddot\psi\right)E*\Big]$$

$$-e\sin(\theta+\phi)\Big[\left(\cos\psi\dot\psi^2+\cos\psi\dot\beta^2+\cos\psi\dot\zeta^2+\sin\psi\ddot\zeta+2\cos\psi\dot\psi\dot\zeta+\sin\psi\ddot\psi\right)x\Big]$$

$$+(k_{m_2}^2-k_{m_1}^2)\cos\theta\sin\theta\Big[-\cos\psi\ddot\zeta+2\sin\psi\dot\psi\dot\zeta+\sin\psi\dot\psi^2+\sin\psi\dot\zeta^2-\cos\psi\ddot\psi\Big]$$

$$+(k_{m_2}^2\sin^2\theta+k_{m_1}^2\cos^2\theta)\Big[2\sin\psi\dot\psi\dot\beta-\cos\psi\ddot\beta\Big]\Big\}$$

$$+mw'\Big\{e\cos\theta\Big[-\sin\psi\ddot v-2\left(\cos\psi\dot\zeta+\cos\psi\dot\psi\right)\dot v-2\cos\psi\dot\beta\dot w+$$

$$\left(2\sin\psi\dot\psi\beta\dot\beta+2\sin\psi\dot\psi\zeta\dot\zeta-\cos\psi\beta\ddot\beta-\cos\psi\zeta\ddot\zeta+\sin\psi\dot\psi^2\zeta+\sin\psi\,\zeta\dot\zeta^2-\cos\psi\ddot\psi\zeta\right)x$$

$$-\left(\cos\psi\ddot\zeta-2\sin\psi\dot\psi\dot\zeta-\sin\psi\dot\psi^2-\sin\psi\dot\zeta^2+\cos\psi\ddot\psi\right)v+\left(2\sin\psi\dot\psi\dot\beta-\cos\psi\ddot\beta\right)w$$

$$-\left(\sin\psi\ddot\zeta+\cos\psi\dot\psi^2+\cos\psi\dot\beta^2+\cos\psi\dot\zeta^2+2\cos\psi\dot\psi\dot\zeta+\sin\psi\ddot\psi\right)(P+L)$$

$$-\left(\cos\psi\dot\psi^2+\cos\psi\dot\beta^2+\sin\psi\ddot\psi\right)F-\left(\cos\psi\dot\psi^2+\sin\psi\ddot\psi\right)E*\Big]$$

$$-e\cos(\theta+\phi)\Big[\left(\sin\psi\ddot\psi+\cos\psi\dot\psi^2+\cos\psi\dot\beta^2+\cos\psi\dot\zeta^2+\sin\psi\ddot\zeta+2\cos\psi\dot\psi\dot\zeta\right)x\Big]$$

$$+(k_{m_2}^2-k_{m_1}^2)\cos\theta\sin\theta\Big[2\sin\psi\dot\psi\dot\beta-\cos\psi\ddot\beta\Big]$$

$$+(k_{m_2}^2\cos^2\theta+k_{m_1}^2\sin^2\theta)\Big[-\cos\psi\ddot\zeta+2\sin\psi\dot\psi\dot\zeta+\sin\psi\dot\psi^2+\sin\psi\dot\zeta^2-\cos\psi\ddot\psi\Big]\Big\}$$

(B-4)

The following calculations include blade mass and geometrical constants using the definitions in the previous sections. The calculated values below are based on properties of an aluminium 2026-T6 NACA0012 airfoil as mentioned, with a chord length of 7.53 cm and an average skin thickness of 1.5 mm, as shown in Fig C-1. The blade mass and geometrical constants are:

$$m = 0.5788\frac{kg}{m} \qquad e = 1.722 \times 10^{-12}m \qquad k_{m_1}^2 = 7.217 \times 10^{-7}m^2 \qquad k_{m_2}^2 = 4.094 \times 10^{-4}m^2$$

$$k_m^2 = 4.101 \times 10^{-4}m^2 \qquad A = 2.090 \times 10^{-4}m^2 \qquad e_A = 1.053 \times 10^{-11}m \qquad k_A^2 = 4.101 \times 10^{-4}m^2$$

$$EI_{y'} = 10.56Nm^2 \qquad EI_{z'} = 5.988 \times 10^3 Nm^2 \qquad GJ = 3.047 \times 10^2 Nm^2$$

$$B_1 = 9.440 \times 10^{-11}m^6 \qquad B_2 = 4.634 \times 10^{-8}m^5$$
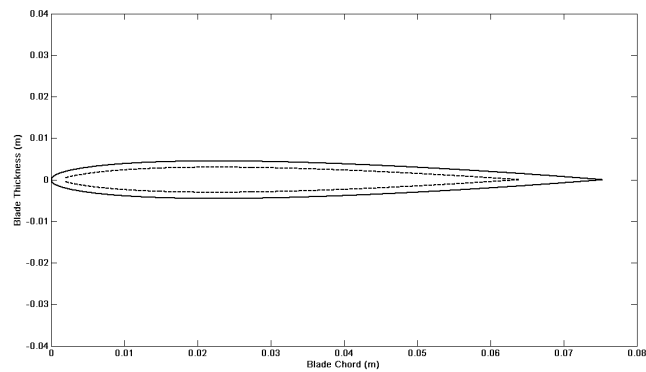
$$C_1 = 0 \qquad C_2 = 0$$

Figure C-1: Blade cross section used to calculate constants